Wear xxx (2011) xxx–xxx

Contents lists available at SciVerse ScienceDirect

Wear

journal homepage: www.elsevier.com/locate/wear

A statistical model for material removal prediction in polishing

X.L. Jin, L.C. Zhang*

School of Mechanical and Manufacturing Engineering, The University of New South Wales, NSW 2052, Australia

ARTICLE INFO

Article history:
Received 10 March 2011
Received in revised form 20 August 2011
Accepted 23 August 2011
Available online xxx

Keywords:
Polishing
Polishing pad
Contact mechanics
Abrasion wear
Material removal
Statistical theory
Chemo-mechanical polishing

ABSTRACT

This paper develops analytically a statistical model for predicting the material removal in mechanical polishing of material surfaces (MS). The model was based on the statistical theory and the abrasive–MS contact mechanisms. The pad-MS and pad-abrasive-MS interactions in polishing were characterised by contact mechanics. Two types of active abrasive particles in the polishing system were considered, *i.e.*, Type I – the particles that can slide and rotate between the pad and MS, and Type II – those embedded in the pad without a rigid body motion. Accordingly, the material removal is considered to be the sum of the contributions from the two types of abrasive interactions. It was found that the mechanical properties and microstructure of the polishing pad and polishing conditions have a significant effect on the material removal rate, such as the porosity and elastic modulus of the pad, polishing pressure, volume concentration of abrasives, particle size, pad asperity radius and pad roughness. It was also found that different types of active particles contribute quite differently to the material removal. When the mean particle radius is small, the material removal is mainly due to the Type II particles, but when the mean particle radius becomes large, the Type I particles remove more materials. The model predictions are well aligned with experimental results available in the literature and can be used for the material removal prediction in chemo-mechanical polishing if a proper treatment of the chemical effect is introduced.

1. Introduction

Mechanical polishing using abrasive slurry is a key finishing process in industry for producing a material surface (MS) of low surface roughness. Chemo-mechanical polishing (CMP) is a good example that is based on mechanical polishing, but introduces chemical reaction by adding chemicals to abrasive slurry to promote the material removal rate. The technique has been widely used in polishing glass, silicon and ceramic surfaces as well as in planarizing surfaces of inter-level dielectrics or inter-metal dielectrics during integrated circuit fabrication [1–5]. In a typical CMP process, a rotating material surface (MS) attached to a carrier is pressed against a rotating polishing pad in the presence of liquid slurry which contains abrasive particles with chemicals. The material removal of the process is generally due to the combination of erosion and abrasion. It is known that many variables such as applied normal force, relative velocity of the MS to the pad, pad properties (elastic modulus, hardness, etc.) and slurry characteristics, have profound influences on the material removal mechanically. The fundamental mechanisms of the material removal in the process are very complicated and have not been well understood, because of the statistical nature of the surfaces in contact such as the random distributions of the surface asperities and abrasive particles.

In the literature, the modelling of the material removal in CMP processes can be generally classified into two categories. One was based on fluid hydrodynamics. For example, Runels et al. [6,7] obtained the wear rate by numerically solving the Navier–Stockes equation. Sumdrarajian et al. [8] studied the removal rate based on the lubrication and mass transport models, in which slurry erosion was considered a main mechanism. The other group of the modelling methods was based on the theory of contact mechanics. Since this approach is more plausible to describe experimental observations, it has been widely accepted and investigated. Larsen-basse and Liang [9] concluded that material removal in CMP is due to particle abrasion. There are also some similar investigations. Luo and Dornfeld [10] investigated the abrasion mechanism in solid–solid mode of the CMP process based on a number of assumptions: plastic wafer–abrasive and pad–abrasive contacts, normal distribution of abrasive size and periodic roughness of pad surface. They extended the model as a function of the abrasive weight concentration [11] and then further used it to explain the effects of abrasive size distribution [12]. However, these models were based on the assumption of periodic roughness of pad surface. From the perspective of pad modelling, abrasive behaviour and distribution effects of abrasive, Wang et al. [13] presented three models for material removal to try to understand how particle properties in conjunction with pad information influence material removal rate.

* Corresponding author. Tel.: +61 2 93856078; fax: +61 2 9385 7316.
E-mail address: Liangchi.Zhang@unsw.edu.au (L.C. Zhang).

0043-1648/$ – see front matter © 2011 Elsevier B.V. All rights reserved.
doi:10.1016/j.wear.2011.08.028

Nomenclature

A_0	nominal area of contact between pad and material surface
A_1	total contact area by Type I particles
A_2	total contact area by Type II particles
A_c	total contact area in a polishing process
A_d	total direct contact area between the pad and material surface
$\tilde{A}_1$	area of asperity contact due to Type I particles
$\tilde{A}_2$	area of asperity contact due to Type II particles
d	separation of the reference planes of Surface 1 and Surface 2 (pad)
E_2	elastic modulus of a pad
E'	composite elastic modulus $E' = E_2/(1-\nu_2^2)$
G_1	wear volume of the material due to Type I particles
G_2	wear volume of the material due to Type II particles
$\tilde{G}$	wear volume of the material by an individual active particle
H_w	hardness of a workpiece material
K	wear coefficient
M_1	material removal rate due to Type I particles
M_2	material removal rate due to Type II particles
M_r	total material removal rate
p_0	polishing pressure
R_p	average asperity radius of a pad
P_1	total contact force on Type I particles
P_2	total contact force on Type II particles
P_d	direct contact force between the pad and material surface
$\tilde{P}_1$	contact force of Type I particles
$\tilde{P}_2$	contact force of Type II particles
r	particle radius
t	polishing time
u_r	mean particle radius
V	pad/material sliding velocity
x	particle volume concentration of slurry
z_2	asperity height of Surface 2 (pad)
α	porous coefficient
η_v	number of particles per unit volume of slurry
η_p	surface density of asperity on Surface 2 (pad)
σ_r	standard deviation of particle radius
σ_p	standard deviation of pad asperity height
$\phi_r(r)$	probability density function of particle size
$\phi(z_2)$	probability density function of pad asperity height
ν_2	Poisson's ratio of a pad

Zhao and Chang [14] studied the material removal rate based on the elastic–plastic micro-contact mechanics and abrasion wear, where the chemical effect was claimed to have been formulated by introducing a density ratio of a chemical thin film. Oh and Seok [15] proposed a model for silicon dioxide CMP based on a multi-scale mechanical abrasion consideration and coupled with the effect of the slurry chemical diffusion. Bozkaya and Muftu [16] investigated the material removal with two-body pad–wafer and three-body pad–abrasive–wafer contacts, and introduced a thin passivated layer on the wafer surface to take into account the effect of chemical reactions between slurry and wafer. Some researchers have also studied the wear mechanisms and material removal rates in CMP processes based on the combination of the above two approaches, *i.e.*, contact mechanics and fluid hydrodynamics [17–20]. To our knowledge, most existing studies only consider the particles embedded in the pad as the active particles. In reality, however, many active particles also slide and rotate between the pad and wafer, as pointed out by Zhang and Tanaka [21]. Therefore, some critical questions naturally arise: How do the two types of active particles contribute to the material removal and how do their contributions vary with the change of polishing conditions when the particle size and distribution are random?

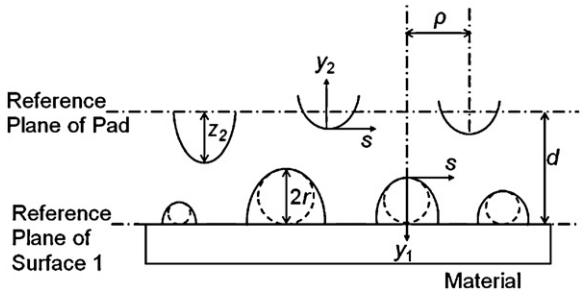

Fig. 1. The contact model of Type I particles, where the dashed circles indicate particles and the solid curves stand for asperities.

This paper will try to answer these questions by developing a statistical model for predicting the material removal in mechanical polishing where both the polishing pad surface and the particle size are random. The investigation will be based on the abrasion wear and contact mechanics of pad–MS and pad–abrasive–MS interactions.

2. Modelling

Assume that the material removal from a surface is caused by abrasion wear by the abrasive particles in polishing slurry. The polishing pressure applied on the MS, p_0, is carried by two kinds of contacts. One is the three-body contact of the pad, the abrasive particles and the MS (*particle contact*); and the second is the two-body contact directly between the pad and the MS (*direct contact*). In the scenario of the particle contact, the particles can be divided into two types, *i.e.*, Type I – the particles can slide and rotate between the pad and MS, and Type II – the particles are embedded in the polishing pad so that they could not have any rigid body motion. The aim of our modelling below is to formulate the material removal rate (MRR) considering the key parameters including the porosity and elastic modulus of polishing pad, pressure, abrasive volume concentration and size, and pad asperity radius and roughness. In addition to the above, the modelling below will consider the random nature of the particle size and polishing pad surface. Thus the model to be developed will be statistical, which will better mimic a real polishing process. The model will also avoid the problems in the literature which mostly assume a uniform particle size and are based on a deterministic material removal mechanism in the modelling. However, as has been validated by the previously in the literature [10–14], the formulation in the present work will consider that the contact is static and the polishing pressure is constant.

2.1. Particle contact and direct contact

2.1.1. Modelling the particle contact

As discussed previously, there are two types of particle contacts. The Type I particles can slide and rotate between the pad and MS. For convenience, these particles can be regarded as the additional asperities to define a new MS. If we assume that the particle radius (hence the asperity radius) is r, then the contact in this case becomes that between the new MS surface and the pad surface—the contact between two rough surfaces, as illustrated in Fig. 1. It should be noted that the asperity height of the pad is less than the separation d of the reference planes of the two rough surfaces. The contact

Please cite this article in press as: X.L. Jin, L.C. Zhang, A statistical model for material removal prediction in polishing. Wear (2011), doi:10.1016/j.wear.2011.08.028

between the two rough surfaces can be generally described by the Greenwood-Tripp model [22], as briefed below. Assume that the new rough surface is Surface 1 and that of the pad is Surface 2. If the asperity shapes of the two rough surfaces are $y_1(s) = s^2/2r$ and $y_2(s) = s^2/2R_p$, where subscript i ($i = 1, 2$) denotes Surface i, R_p is the average asperity radius of the pad, and s is the local coordinate of the asperity. The pairs of asperities are not aligned generally. The contact point of the asperity pair on the two surfaces is situated at a distance $r_1 = \rho r/(r + R_p)$ from the centre of the asperity on Surface 1 and a distance $r_2 = \rho R_p/(r + R_p)$ from the centre of the asperity on Surface 2, in which ρ is the distance of the asperities of the two surfaces. Based on the Hertzian theory, the asperity contact behaviour can be expressed as follows

$$\begin{aligned} \tilde{A}_1 &= \pi R w \\ \tilde{P}_1 &= \frac{4}{3} E' R^{1/2} w^{3/2} \end{aligned} \tag{1}$$

where the equivalent radius R and the composite elastic modulus E' are given by $1/R = 1/r + 1/R_p$ and $1/E' = (1 - \nu_1^2)/E_1 + (1 - \nu_2^2/E_2)$, respectively. The interference at the contact is $w = 2r + z_2 - d - r_1^2/2r - r_2^2/2R_p = 2r + z_2 - d - \rho^2/2(r + R_p)$, in which z_2 is the asperity height of Surface 2. Since a polishing pad is usually much softer than the abrasive particle and workpiece materials, the composite elastic modulus can be simplified to $E' = E_2/(1 - \nu_2^2)$, where E_2 and ν_2 are the solid pad elastic modulus and Poisson's ratio, respectively. Assume that the abrasive particles are spherical and the probability density function of the particle size is $\phi_r(r)$. Then, the average volume of the abrasive particle is $\int_0^\infty 4/3\pi r^3 \phi_r(r) dr$. On the basis of the definition of the abrasive volume concentration, the number of particles per unit volume of the slurry, η_v, can be computed by the following expression,

$$\eta_v = \frac{x}{\int_0^\infty 4/3\pi r^3 \phi_r(r)\ dr} \tag{2}$$

where x is the abrasive volume concentration of the slurry. With η_v defined, the number of asperities in the range r to $r + dr$ situated between ρ and $\rho + d\rho$ from one asperity on Surface 2 can be calculated as $2r\eta_v \cdot 2\pi\rho \mathrm{d}\rho\phi_r(r)dr$. There are $\eta_p A_0 \phi(z_2) dz_2$ asperities on Surface 2 with heights between z_2 and $z_2 + dz_2$, where η_p is the surface density of asperity on Surface 2, $\phi(z_2)$ is the probability density function of the pad asperity height and A_0 is the nominal area of contact between pad and MS. Therefore, the expected number of contacts can be obtained as

$$n_{c_1} = 2\pi\eta_p\eta_v A_0 \int_r \int_{z_2} \int_\rho 2r\rho\phi(z_2)\phi_r(r) d\rho\, dz_2 dr \tag{3}$$

Similarly, based on the statistical theory, the expected total area A_1 and force P_1 associated with the Type I contact are

$$\begin{aligned} A_1 &= 2\pi\eta_p\eta_v A_0 \int_r \int_{z_2} \int_\rho 2r\tilde{A}_1 \rho\phi(z_2)\phi_r(r) d\rho dz_2 dr \\ P_1 &= 2\pi\eta_p\eta_v A_0 \int_r \int_{z_2} \int_\rho 2r\tilde{P}_1 \rho\phi(z_2)\phi_r(r) d\rho dz_2 dr \end{aligned} \tag{4}$$

It should be pointed out that here $\rho r/(r + R_p) \le 2r$ and $z_2 \le d$. Then, substituting Eq. (1) into Eq. (4) results in

$$\begin{aligned} A_1 &= 2\pi^2\eta_p\eta_v A_0 \int_0^\infty \int_{d-2r}^{d} r^2 R_p (z_2 + 2r - d)^2 \phi(z_2)\phi_r(r) dz_2 dr \\ P_1 &= 32/15\pi\eta_p\eta_v A_0 \int_0^\infty \int_{d-2r}^{d} r\sqrt{rR_p(r + R_p)}(z_2 + 2r - d)^{5/2}\phi(z_2)\phi_r(r) dz_2 dr \end{aligned} \tag{5}$$

Now let us consider the Type II particles which are embedded in the pad without a rigid body motion. Again the asperity height of the pad is larger than d. Assume that the particle-pad deformation is elastic. As the indentation into the MS by an active particle is very small [23] and is negligible compared with that into the pad, for simplicity we assume that the indentation into the pad is $2r$. This gives rise to

$$\begin{aligned} \tilde{A}_2 &= 2\pi R r \\ \tilde{P}_2 &= \frac{4}{3} E' R^{1/2} (2r)^{3/2} \end{aligned} \tag{6}$$

The area that the particles could be embedded in the pad is $\eta_p A_0 \int_d^\infty \pi R_p (z_2 - d)\phi(z_2) dz_2$. Thus the expected number of the contacts in this case can be described by

$$n_{c_2} = \eta_p\eta_v A_0 \int_d^\infty \pi R_p (z_2 - d)\phi(z_2) dz_2 \int_0^\infty 2r\phi_r(r) dr \tag{7}$$

The expected total area A_2 and force P_2 for the Type II contact are therefore

$$\begin{aligned} A_2 &= 4\pi^2\eta_p\eta_v R_p A_0 \int_d^\infty (z_2 - d)\phi(z_2) dz_2 \int_0^\infty r^3 R_p/(r + R_p)\phi_r(r)\ dr \\ P_2 &= \frac{4}{3} E'\pi\eta_p\eta_v R_p A_0 \int_d^\infty (z_2 - d)\phi(z_2) dz_2 \int_0^\infty (2r)^{5/2}\sqrt{rR_p/(r + R_p)}\phi_r(r)\ dr \end{aligned} \tag{8}$$

2.1.2. Modelling the direct contact

Unlike the scenario of particle contact discussed in the last section, in the characterisation of the direct contact, the MS can be regarded as a smooth plane because the MS is much smoother than the polishing pad. Thus the GW model can be applied [24]. If there is no particle, the total contact area and force between the pad and MS are

$$\begin{aligned} A_d &= \pi\eta_p R_p A_0 \int_d^\infty (z_2 - d)\phi(z_2) dz_2 \\ P_d &= \frac{4}{3}\eta_p R_p^{1/2} E'' A_0 \int_d^\infty (z_2 - d)^{3/2}\phi(z_2) dz_2 \end{aligned} \tag{9}$$

where $E'' = \alpha E'$ and $\alpha (0 < \alpha \le 1)$ is the porous coefficient introduced to capture the effect of the porous surface structure of the pad (the smaller the α, the more porous of the pad). When there are embedded particles on the pad surface, *i.e.*, Type II particles, it is reasonable to assume that the actual pressure remains the same as that in the case without a particle. Therefore, the real direct contact area A_d and force P_d in this case are

$$\begin{aligned} A_d &= \pi\eta_p R_p A_0 \int_d^\infty (z_2 - d)\phi(z_2) dz_2 - A_2 \\ P_d &= \frac{4E'' \int_d^\infty (z_2 - d)^{3/2}\phi(z_2) dz_2}{3\pi R_p^{1/2} \int_d^\infty (z_2 - d)\phi(z_2) dz_2} A_d \end{aligned} \tag{10}$$

It should be pointed out that physically $A_d \ge 0$.

The total contact area A_c between MS and pad with abrasive particles can be obtained by $A_c = A_d + (P_1 + P_2)/H_w$, where H_w is the hardness of the workpiece material. Generally, A_c is dominated by A_d and the force balance equation can be obtained as follows,

$$P_1 + P_2 + P_d = p_0 A_0 \tag{11}$$

From Eq. (11), the separation d can be calculated.

2.2. Material removal

As aforementioned, the material removal from the materials is due to abrasion wear by both the Type I and Type II particles. Consider a single particle contact between the pad and MS illustrated in Fig. 2. Based on the wear mechanism, the wear volume of the material by an individual active particle is

$$\tilde{G} = K\tilde{S}Vt \tag{12}$$

Please cite this article in press as: X.L. Jin, L.C. Zhang, A statistical model for material removal prediction in polishing. Wear (2011), doi:10.1016/j.wear.2011.08.028

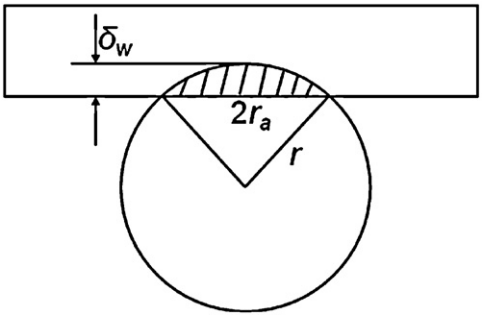

Fig. 2. A particle in contact with the MS.

where $\tilde{S}$ is the cross-sectional area of the worn groove in the MS generated by the active particle, *i.e.*, the shaded area in Fig. 2, V is the pad/material sliding velocity, t is the polishing time and K is the wear constant. $\tilde{S}$ can be determined by

$$\tilde{S} = r_a \delta_w \tag{13}$$

where r_a is the radius of the contact area between the active particle and the MS and δ_w is the indentation depth of the particle into the MS. It is noticed that $r_a^2 = 2r\delta_w$ and $\tilde{P}_p = H_w \pi r_a^2$, where $\tilde{P}_p$ is the particle contact force and can be either $\tilde{P}_1$ or $\tilde{P}_2$. Then Eq. (13) can be rewritten as

$$\tilde{S} = \left(\frac{\tilde{P}_p}{\pi H_w}\right)^{3/2} \frac{1}{2r} \tag{14}$$

By using Eqs. (12) and (14), the wear of the material by Type I contact, G_1, is

$$G_1 = \frac{KA_0Vt}{(H_w)^{3/2}} M_1 \tag{15}$$

where

$$M_1 = \frac{8}{13}\pi\eta_p\eta_v\left(\frac{4E'}{3\pi}\right)^{3/2} \int_0^{\infty}\int_{d-2r}^{d} \left(\frac{rR_p}{r+R_p}\right)^{3/4} (r+R_p)(z_2+2r-d)^{13/4}\phi(z_2)\phi_r(r)\,dz_2 dr \tag{16}$$

For the Type II contact, the wear of the material G_2 is similar to Eq. (15) except that M_1 in the equation is replaced by M_2 below

$$M_2 = \pi\eta_p\eta_v R_p\left(\frac{4E'}{3\pi}\right)^{3/2} \int_d^{\infty}(z_2-d)\phi(z_2)dz_2 \int_0^{\infty}\left(\frac{rR_p}{r+R_p}\right)^{3/4} (2r)^{9/4}\phi_r(r)\,dr \tag{17}$$

Then the total MRR M_r can be derived from the total wear of the material in the process, *i.e.*, the summation of the wear by both Type I and Type II contacts, given by

$$M_r = \frac{G_1+G_2}{A_0 t} = \frac{KVM}{(H_w)^{3/2}} \tag{18}$$

where $M = M_1 + M_2$. It can be seen from Eq. (18) that with given K, V and H_w, the MRR is solely determined by M.

It should be pointed out that K and V reflect the average contributions of polishing velocity and fluid dynamics; or in other words, they accommodate the effect of particle kinematics and fluid dynamics indirectly in the present material removal model. Moreover, it is known that chemicals in the slurry of a chemo-mechanical polishing process can alter the hardness of the workpiece material. Thus, if the chemical effect is considered in the material removal, an effective hardness should be introduced to replace H_w in Eq. (18).

Table 1
Parameter variation ranges.

Parameter	Primary value	Range
Polishing pressure, p_0	0.02 MPa	0–0.1 MPa
Abrasive volume concentration, x	2.5%	0.1–10.1%
Mean particle radius, u_r	25 nm	25-10025 nm
Standard deviation of particle radius, σ_r	$u_r/5$	
Pad asperity density, η_p	$2\times10^{-4}/\mu m^2$	
Pad asperity radius, R_p	50 μm	25–105 μm
Standard deviation of pad asperity height, σ_p	5 μm	1–21 μm
Solid pad elastic modulus, E_2	5 MPa	3 MPa, 5 MPa
Solid pad Poisson's ratio, ν_2	0.49	
Coefficient, α	0.25	0.25,1

It should be noted that the determination of the effective hardness is out of the scope of the present study.

3. Results and discussion

As a special case, assume that both $\phi(z_2)$ and $\phi_r(r)$ are Gaussian, *i.e.*, $\phi(z_2) = \exp(-z_2^2/2\sigma_p^2)/(\sqrt{2\pi}\sigma_p)$ and $\phi_r(r) = \exp(-(r-u_r)^2/2\sigma_r^2)/(\sqrt{2\pi}\sigma_r)$, where σ_p is the standard deviation of pad asperity height, u_r is the mean particle radius and σ_r is the standard deviation of particle radius. The MRR can therefore be obtained by the model of Eq. (18). With this model, in addition to the effects of the porosity and elastic modulus of the pad, polishing pressure, volume concentration of abrasives, mean particle radius, pad asperity radius and pad roughness, we can also investigate the contributions of these parameters to M_1 and M_2 individually. The primary parameter values used for the model calculation and their variation ranges used for examining the effect of each parameter are listed in Table 1. Hence, if it is not further specified, the parameter values in the model calculation will be from this table. Since K, V and H_w are constants in a given polishing system, we will discuss M in Eq. (18) instead of M_r. For convenience, we still refer to M as MRR in the discussion.

3.1. Effect of polishing pressure

The effect of pressure p_0 on M is shown in Fig. 3 when the property of the polishing pad, elastic modulus E_2 and porous coefficient α change. It can be seen that the MRR is nearly proportional to the

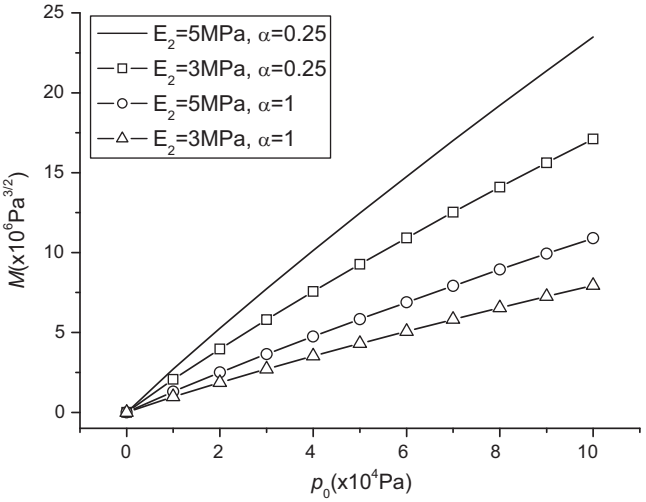

Fig. 3. Variation of material removal rate (M) with polishing pressure and pad properties.

Please cite this article in press as: X.L. Jin, L.C. Zhang, A statistical model for material removal prediction in polishing. Wear (2011), doi:10.1016/j.wear.2011.08.028

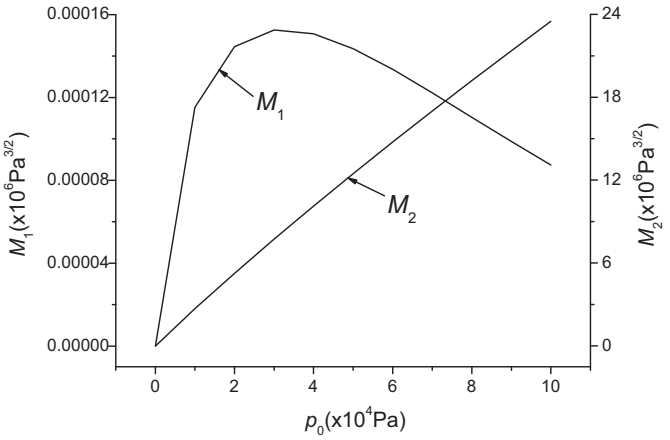

Fig. 4. The effect of the polishing pressure on M_1 and M_2.

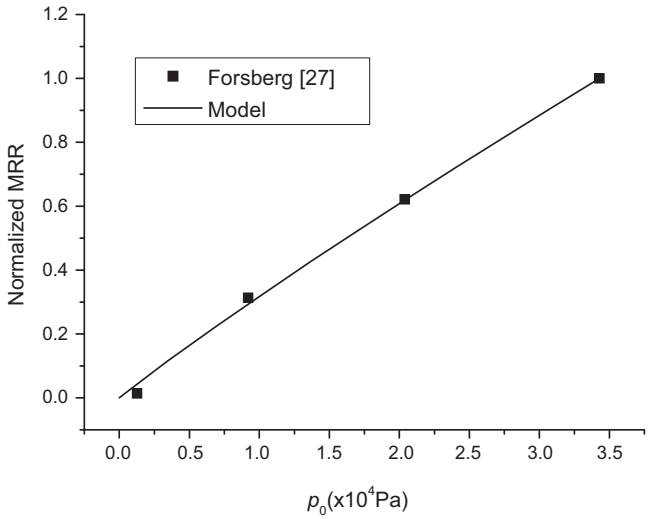

Fig. 5. Variation of normalized MRR with polishing pressure p_0.

applied pressure. Both the pad elastic modulus and porosity alter the MRR. A larger E_2 (hence a harder pad) or a smaller α (hence a more porous pad) will lead to a larger MRR. This is in agreement with the observations by Bozkaya and Muftu [16], and can be understood as follows: For a harder pad, the particle contact force becomes larger and then the indentation into the MS by an active particle increases, causing the MRR to increase. While with a more porous pad, the deformation of the pad asperities in polishing can be larger, *i.e.*, the separation d becomes smaller, leading to more active particles in contact with the workpiece and in turn bringing about a greater MRR.

Fig. 4 shows the effect of the polishing pressure on M_1 and M_2, indicating the contributions of Type I and Type II to the total MRR. It can be found that the MRR is dominated by Type II particles. M_2 increases with the polishing pressure while M_1 increases first but then decreases with the polishing pressure. It is easy to understand that a larger polishing pressure will lead to greater deformation in the polishing system. As a result, the number of the active particles becomes large. When the pressure increases to a certain extent, the Type I particles can become Type II. It is therefore reasonable that the variation of M_1 with p_0 is peaked at certain value of p_0.

The total contact area between MS and pad with abrasive particles predicted by the model is 1.89% at $p_0 = 0.01$ MPa and 4.54% at $p_0 = 0.025$ MPa. They are smaller than the corresponding 5% and 7.19% experimentally measured [25]. This is reasonable because Zhang, Biddut and Ali [25] used a colour coating method to record the contact area, which has a low resolution, cannot accurately eliminate the small valleys, and hence overestimates the total contact area. Using their experimental data at polishing pressures of $p_0 = 0.01$ MPa, $p_0 = 0.02$ MPa and $V = 0.17$ m/s [26], the average wear coefficient in Eq. (18) is determined to be $K = 3.545$. The model then predicts that the MRR is 0.0575 μm/min under the polishing condition of $H_w = 12.7$ GPa, $V = 0.143$ m/s and $p_0 = 0.01$ MPa, which is in very good agreement with the experimental result of 0.075 μm/min [25] under the same polishing condition. Fig. 5 shows the comparison of the model-predicted MRR with another experiment [27], where the normalized MRR is defined as the MRR normalized by the largest MRR in the range of examination/consideration, *i.e.*, $0 \le p_0 \le 34,300$ Pa. In the calculation using the model, the volume concentration of abrasives x is the same as that used in the experiment and all the parameters are as follows: $x = 2.1\%/2.5$, $u_r = 25$ nm, $\sigma_r = 6.25$ nm, $\eta_p = 2 \times 10^{-4}$ μm, $R_p = 50$ μm, $\sigma_p = 5$ μm, $E_2 = 10$ MPa, $\nu_2 = 0.49$ an $\alpha = 0.25$. In the experiment, MRR is about 3.1 μm/h when $x = 0$ (*i.e.*, when the MRR was solely due to the etching by slurry chemicals). However, such a chemical effect is not directly included in the model. Hence, to make a reasonable comparison between the model prediction and the experimental result, it is necessary to subtract the MRR due to etching at $x = 0$ (*i.e.*, 3.1 μm/h) from all the MRR values experimentally measured before normalisation. It can be seen from Fig. 5 that the model gives excellent predictions. Furthermore, we can also observe that MRR is almost proportional to the applied pressure.

3.2. Effect of abrasive volume concentration

The effect of the abrasive volume concentration x on M is shown in Fig. 6, when the pad elastic modulus E_2 and porous coefficient α change. It can be seen that M increases with the increasing abrasive volume concentration, but eventually approaches a steady state. This is because an increase in abrasive concentration will first result in an increase in the number of active particles. However, a saturation state will be reached when the increase of x makes the direct contact area of pad-workpiece diminish, as shown in Fig. 7. From Eq. (10), such saturation x is $\int_0^\infty r^3\phi_r(r)/3dr / \int_0^\infty r^3 R_p/(r+R_p)\phi_r(r)\,dr$, which depends on the particle size, and pad topography.

The effect of the abrasive volume concentration x on M_1 and M_2 is shown in Fig. 8. Similarly, Type II contact dominates the MRR. Both M_1 and M_2 increase with x due to the increasing number of the active particles.

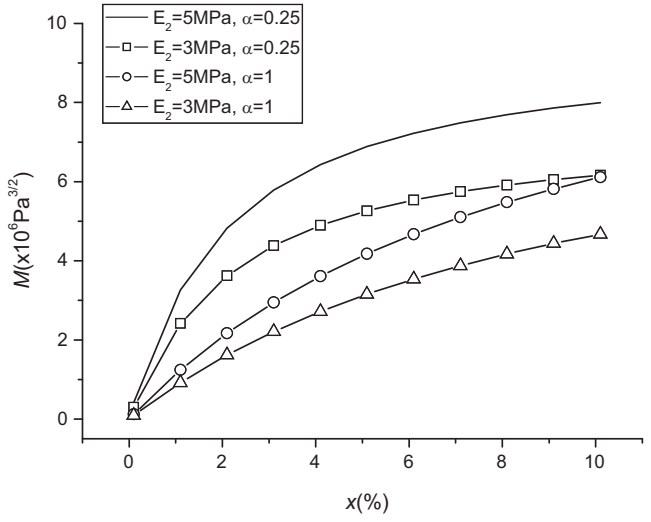

Fig. 6. Variation of M with the abrasive volume concentration and pad properties.

Please cite this article in press as: X.L. Jin, L.C. Zhang, A statistical model for material removal prediction in polishing. Wear (2011), doi:10.1016/j.wear.2011.08.028

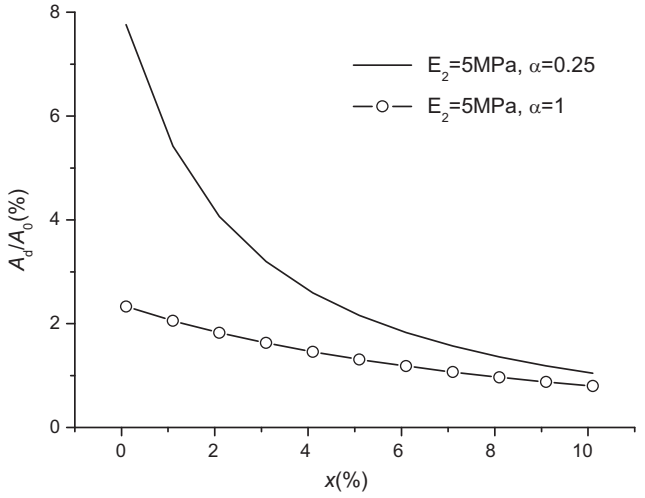

Fig. 7. The direct contact area ratio vs. *x*.

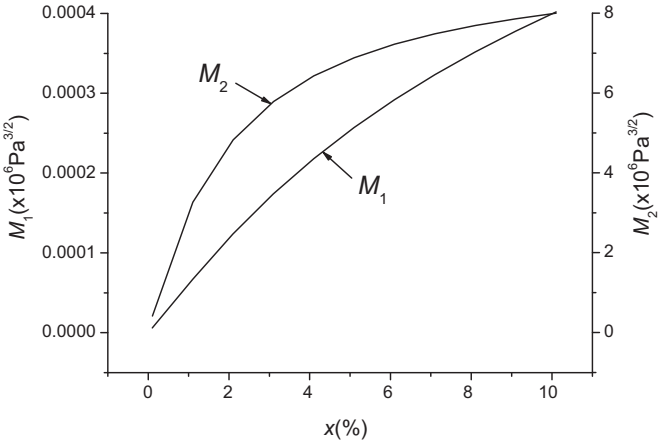

Fig. 8. The effect of the abrasive volume concentration on M_1 and M_2.

Fig. 9 shows the comparison of the normalized MRR from the experiment [27] with the model prediction, when the abrasive volume concentration varies in the range of $0 \le x \le 2.6\%$ under $p_0 = 0.009$ MPa. Similar to the previous comparison in Fig. 5, the MRR due to etching at $x = 0$ in the experiment has been subtracted.

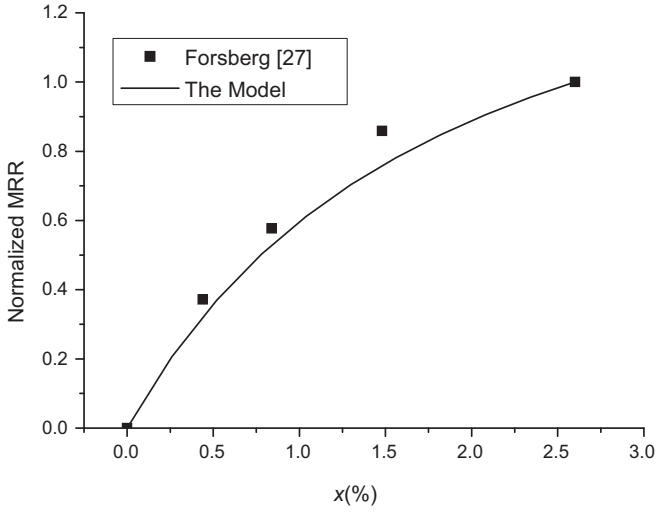

Fig. 9. Variation in the normalized MRR with the abrasive volume concentration.

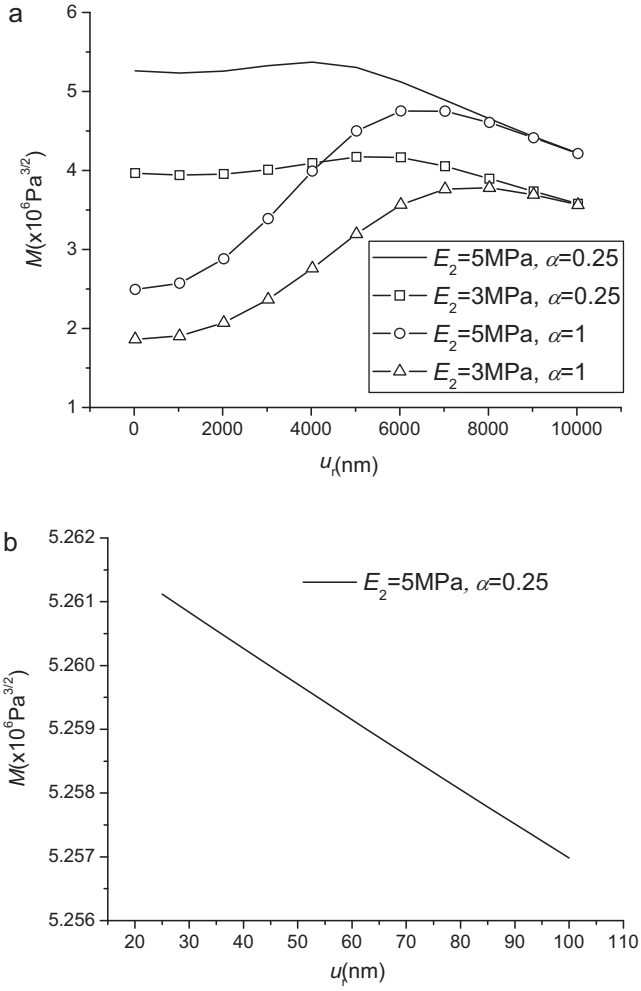

Fig. 10. Variation of *M* with mean particle radius and pad properties.

It can be seen that the model predictions are in excellent agreement with the experimental results.

3.3. Effects of mean particle radius and pad porosity

In addition to the effect of abrasive volume concentration, abrasive particle size in polishing slurry is also of vital importance to the material removal. The effect of the mean particle radius u_r on *M*, as shown in Fig. 10(a), is more complicated. *M* reaches a peak at a critical u_r and then decrease. With a larger u_r, the mean volume of the abrasive particle is larger so that the number of particles per unit volume in the slurry is smaller. As a result, the number of the active particles in contact with the workpiece becomes smaller. On the other hand, the mean particle contact force increases with the increasing mean particle radius. In coupling these effects, hence, the MRR can decrease or increase with the mean particle radius, depending on the relative influence of the individual. When the mean particle radius u_r is small (<100 nm), MRR drops with the increase of u_r, as shown in Fig. 10(b). This means that in this particle size range, the effect of the particle size on the number of the active particles is stronger than that on the mean particle contact force. We noticed that some earlier reports [28,29] on the effect of particle size show contradictory conclusions: Xie et al. [28] found that MRR increases with the particle size, while Bielmann et al. [29] concluded the opposite. The results from the present model clarify this issue: It is the particle size range that makes the MRR variation different, but this range is related to other polishing parameters.

Please cite this article in press as: X.L. Jin, L.C. Zhang, A statistical model for material removal prediction in polishing. Wear (2011), doi:10.1016/j.wear.2011.08.028

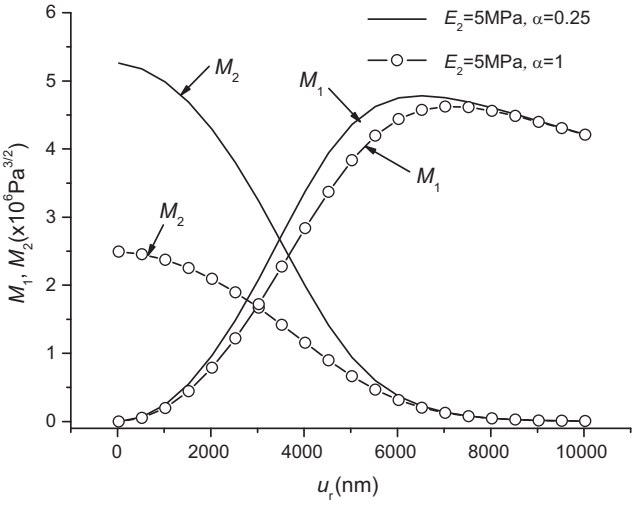

Fig. 11. Effect of the mean particle radius on M_1 and M_2.

Moreover, the analysis using our model emphasises that the relative influence of individual factors determines the coupled effect on MRR.

The pad porosity plays an important role on the MRR. When the mean particle radius u_r is smaller than the critical mean particle, the smaller the porous coefficient α, the flatter the variation of MRR. This can be explained as follows. When the mean particle radius u_r increases, the number of active particles in Type II drops rapidly. Thus M_2 decreases with u_r and finally reduces to zero, as shown in Fig. 11. The effect of the porous coefficient is mainly on the MRR achieved by Type II particles. The more porous the pad is, the more obvious the effect becomes. However, this effect becomes weak when u_r increases. As a result, M_2 decreases more significantly when the pad is more porous. On the other hand, with the increase of u_r, the number of Type I particles first increases and then decrease as has been discussed previously. Therefore, M_1 first increases with u_r and then decreases with it. In a certain range, M_1 increases more quickly due to the additional effect of the particle size on the particle contact force. Thus, in this situation, the variation of the total MRR is slower for more porous pad. It can be found from Fig. 11 that Type II particles dominate the MRR when u_r is smaller but Type I particles play a more important role when u_r is large.

3.4. Effect of pad asperity radius

The surface topography of a rough pad has a strong influence on the contact behaviour in polishing, such as the contact area and contact force, as demonstrated in Fig. 12. Therefore, it is very much worthwhile to understand the effect of the surface topography on M. The results with respect to the pad asperity radius R_p are shown in Fig. 13 with different elastic modulus E_2 and porous coefficient α of the pads. It can be seen that the MRR can be enhanced by using larger pad asperity radius. Similar trend is found in [16]. Fig. 14 shows the effect of R_p on M_1 and M_2. Clearly, Type II particles dominate the MRR. Both M_1 and M_2 increase with the pad asperity radius, and this can be explained by the variation in the number of active particles. As R_p increases, the area that the Type II particles could be embedded in the pad increases, leading to the number of the Type II particles to increase.

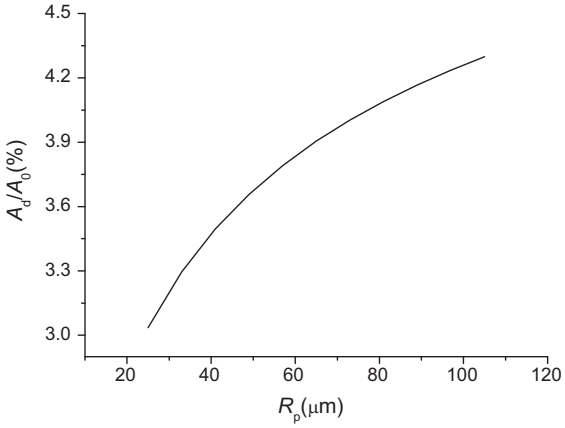

(a) The direct contact area ratio vs R_p

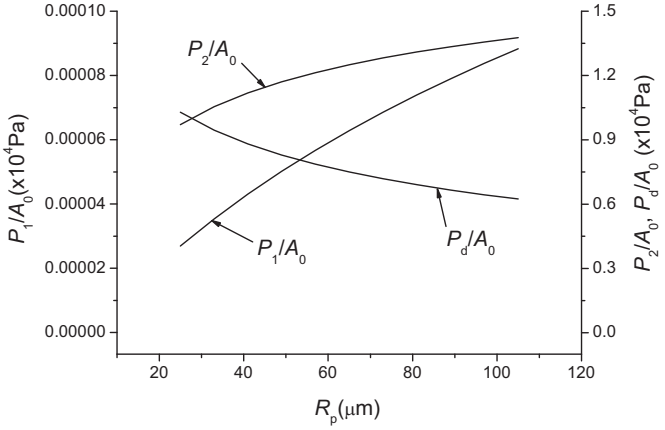

(b) Nominal pressure vs R_p

Fig. 12. Effects of pad asperity radius on the direct contact area and nominal pressure.

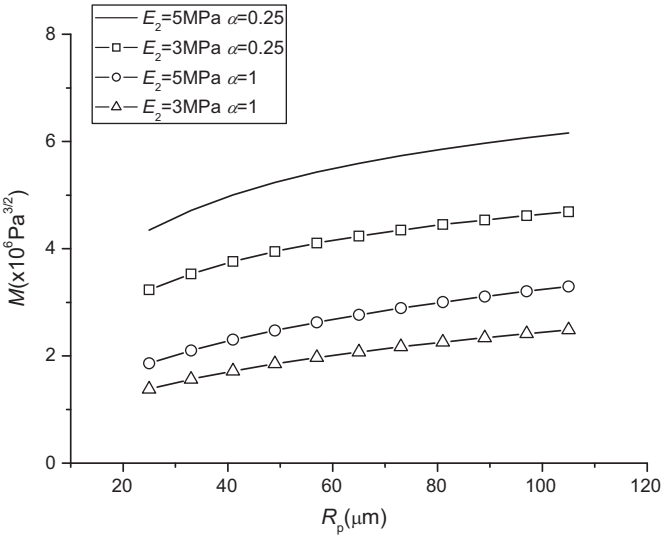

Fig. 13. Variation of M with pad asperity radius and pad property.

Please cite this article in press as: X.L. Jin, L.C. Zhang, A statistical model for material removal prediction in polishing. Wear (2011), doi:10.1016/j.wear.2011.08.028

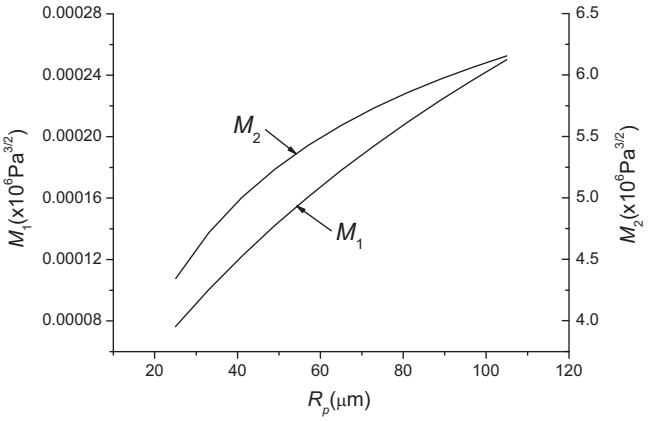

Fig. 14. Effect of pad asperity radius on M_1 and M_2.

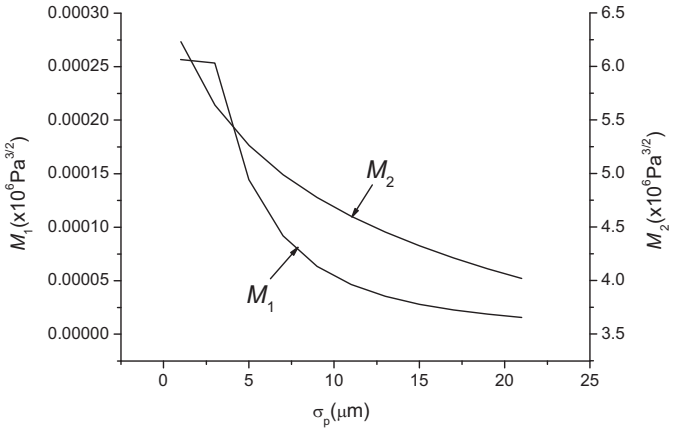

Fig. 16. Effect of the pad roughness on M_1 and M_2.

3.5. Effect of pad roughness

Another quantity related to pad topography, pad roughness, is also influential to the MRR of a polishing system. Fig. 15 shows the effect of the standard deviation of pad asperity height σ_p which is a description of pad roughness. A smaller σ_p means a smoother pad, capable of holding a greater number of active particles. Therefore, it is reasonable to see from Fig. 15 that M decreases with increasing σ_p. It is also found that the larger the E_2 or the smaller the α is, the larger the MRR becomes. Using different pad conditioning methods, Park and Jeong [30] investigated experimentally the effect of pad topographies with $\sigma_p = 4.94\,\mu m$ and $\sigma_p = 2.96\,\mu m$ using silica slurry. They reported that the average MRR achieved using the $\sigma_p = 4.94\mu m$ pad was 10% lower than that by using the $\sigma_p = 2.96\mu m$ pad. Our model predicts that the MRR difference using these two pads is 10.5%, which is in excellent agreement with the experiment [30]. In the model prediction, we have used the same polishing conditions described by [30] quantified by Bozkaya and Muftu [16], except that we used the correct density value of silica in calculation. Fig. 16 shows the effect of the pad roughness on M_1 and M_2 individually, demonstrating that the Type II particles dominate the MRR but that both M_1 and M_2 decrease with increasing the pad roughness.

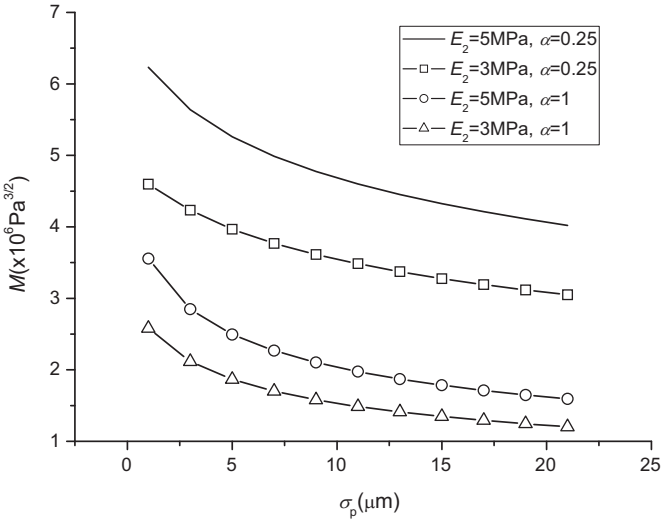

Fig. 15. Variation of M with pad roughness and property.

4. Conclusions

This paper presents a statistical model for the prediction of material removal rate in mechanical polishing of materials. The contact interactions in the polishing process are characterised by the contact mechanics of pad–MS and pad–abrasive–MS interactions. In the pad–abrasive–MS contact, two types of active abrasive particles are considered, *i.e.*, Type I – the particles able to slide and rotate between the pad and MS, and Type II – those embedded in the pad without a rigid body motion. The model has been comprehensively verified by experimental results in the literature. This predictive model enables a detailed investigation into the effects of many key polishing parameters on the MRR, including polishing pressure, abrasive volume concentration and abrasive particle size of polishing slurry, and elastic modulus, surface topography and porosity of a polishing pad.

The analysis with the aid of this model has led to the following major findings:

(1) MRR increases monotonically with the abrasive volume concentration. However, there is a critical volume concentration beyond which a saturation state will be reached. In other words, when the abrasive volume concentration reaches a critical value, MRR will become a constant. Pad surface topography and particle size distribution will influence the critical volume concentration value in a polishing process.
(2) MRR varies with the mean particle radius. It is the range of the particle size distribution that makes the MRR vary in a different manner, increasing or decreasing. This elucidates the conflicting experimental conclusions in the literature. Our analysis also demonstrates that the relative influence of individual polishing parameters determines the coupled effect on MRR.
(3) When the mean particle radius is small, MRR is mainly due to Type II particles; however, when the mean particle radius becomes large, MRR is mainly due to Type I particles.
(4) MRR increases with increasing the pad asperity radius and decreases with the increase of the pad roughness. A harder or a more porous pad will lead to a larger MRR.

Acknowledgement

The work presented in this paper is supported by ARC.

References

[1] M.A. Martinez, Chemical–mechanical polishing: route to global planarization, Solid State Technol. 37 (5) (1994) 26–31.

Please cite this article in press as: X.L. Jin, L.C. Zhang, A statistical model for material removal prediction in polishing. Wear (2011), doi:10.1016/j.wear.2011.08.028

[2] J.M. Steigerwald, S.P. Murarka, R.J. Gutmann, Chemical Mechanical Planarization of Microelectronic Materials, Wiley-VCH, New York, 1997.
[3] I. Zarudi, L.C. Zhang, Subsurface damage in single-crystal silicon due to grinding and polishing, J. Mater. Sci. Lett. 15 (7) (1996) 586–587.
[4] L.C. Zhang, I. Zarudi, An understanding of the chemical effect on the nano-wear deformation in mono-crystalline silicon components, Wear 225–229 (1999) 669–677.
[5] S.H. Li, R.O. Miller, Chemical–Mechanical Polishing in Silicon Processing, Semiconductors and Semimetals, vol. 63, Academic Press, New York, 2000.
[6] S.R. Runnels, L.M. Eyman, Tribology analysis of chemical–mechanical polishing, J. Electrochem. Soc. 141 (6) (1994) 1698–1701.
[7] S.R. Runnels, Feature-scale fluid-based erosion modeling for chemical–mechanical polishing, J. Electrochem. Soc. 141 (7) (1994) 1900–1904.
[8] S. Sundararajan, D.G. Thakurta, D.W. Schwendeman, S.P. Murarka, W.N. Gill, Two-dimensional wafer-scale chemical-mechanical planarization models based on lubrication theory and mass transport, J. Electrochem. Soc. 146 (2) (1999) 761–766.
[9] J. Larsen-Basse, H. Liang, Probable role of abrasion in chemo-mechanical polishing of tungsten, Wear 233–235 (1999) 647–654.
[10] J.F. Luo, D.A. Dornfeld, Material removal mechanism in chemical mechanical polishing: theory and modeling, IEEE Trans. Semicond. Manuf. 14 (2) (2001) 112–133.
[11] J.F. Luo, D.A. Dornfeld, Material removal regions in chemical mechanical planarization for submicron integrated circuit fabrication: coupling effects of slurry chemical, abrasive size distribution and wafer-pad contact area, IEEE Trans. Semicond. Manuf. 16 (1) (2003) 45–56.
[12] J.F. Luo, D.A. Dornfeld, Effects of abrasive size distribution in chemical mechanical planarization: modelling and verification, IEEE Trans. Semicond. Manuf. 16 (3) (2003) 469–476.
[13] C. Wang, P. Sherman, A. Chandra, D. Dornfeld, Pad surface roughness and slurry particle size distribution effects on material removal rate in chemical mechanical planarization, CIRP Ann. Manuf. Technol. 54 (1) (2005) 309–312.
[14] Y.W. Zhao, L. Chang, A micro-contact and wear model for chemical-mechanical polishing of silicon wafers, Wear 252 (2002) 220–226.
[15] S. Oh, J. Seok, An integrated material removal model for silicon dioxide layers in chemical mechanical polishing processes, Wear 266 (2009) 839–849.
[16] D. Bozkaya, S. Muftu, A material removal model for CMP based on the contact mechanics of pad, abrasives, and wafer, J. Electrochem. Soc. 156 (12) (2009) H890–H902.
[17] J. Tichy, J.A. Levert, L. Shan, S. Danyluk, Contact mechanics and lubrication hydrodynamics of chemical–mechanical polishing, J. Electrochem. Soc. 146 (4) (1999) 1523–1528.
[18] J.F. Lin, J.D. Chern, Y.H. Chang, P.L. Kuo, M.S. Tsai, Analysis of the tribological mechanisms arising in the chemical mechanical polishing of copper-film wafers, J. Tribol. Trans. ASME 126 (2004) 185–199.
[19] J. Seok, C.P. Sukam, A.T. Kim, J.A. Tichy, T.S. Cale, Material removal model for chemical-mechanical polishing considering wafer flexibility and edge effects, Wear 257 (2004) 496–508.
[20] C.C. Wei, J.H. Horng, A.C. Lee, J.F. Lin, Analyses and experimental confirmation of removal performance of silicon oxide film in the chemical–mechanical polishing (CMP) process with pattern geometry of concentric groove pads, Wear 270 (2011) 172–180.
[21] L.C. Zhang, H. Tanaka, Atomic scale deformation in silicon monocrystals induced by two-body and three-body contact sliding, Tribol. Int. 31 (8) (1998) 425–433.
[22] J.A. Greenwood, J.H. Tripp, The contact of two nominally flat rough surfaces, Arch.: Proc. Inst. Mech. Eng. 185 (1970) 625–634.
[23] Y.W. Zhao, L. Chang, S.H. Kim, A mathematical model for chemical–mechanical polishing based on formation and removal of weakly bonded molecular species, Wear 254 (2003) 332–339.
[24] J.A. Greenwood, J.B.P. Williamson, Contact of nominally flat surfaces, Proc. R. Soc. Lond. Ser. A 295 (1966) 300–319.
[25] L.C. Zhang, A.Q. Biddut, Y.M. Ali, Dependence of pad performance on its texture in polishing mono-crystalline silicon wafers, Int. J. Mech. Sci. 52 (5) (2010) 657–662.
[26] A.Q. Biddut, Polishing of Silicon Wafer, Ph.D. Thesis, The University of New South Wales, Sydney, in preparation.
[27] M. Forsberg, Effect of process parameters on material removal rate in chemical mechanical polishing of Si(1 0 0), Microelectron. Eng. 77 (2005) 319–326.
[28] Y. Xie, B. Bhushan, Effects of particle size, polishing pad and contact pressure in free abrasive polishing, Wear 200 (1996) 281–295.
[29] M. Bielmann, U. Mahajan, R.K. Singh, Effect of particle size during tungsten chemical mechanical polishing, Electrochem. Solid State Lett. 2 (8) (1999) 401–403.
[30] K. Park, H. Jeong, Investigation of pad surface topography distribution for material removal uniformity in CMP process, J. Electrochem. Soc. 155 (8) (2008) H595–H602.

Please cite this article in press as: X.L. Jin, L.C. Zhang, A statistical model for material removal prediction in polishing. Wear (2011), doi:10.1016/j.wear.2011.08.028